AGU100 ADVANCING EARTH AND SPACE SCIENCE

Earth and Space Science

TECHNICAL REPORTS: METHODS

10.1002/2018EA000372

Special Section:
Planetary Mapping: Methods, Tools for Scientific Analysis and Exploration

Key Points:
- I describe planetary features as fractals, and that fractal nature should be considered in geologic mapping
- I use specific examples of crater ejecta to show that interpretation is very dependent on measuring length scale
- Geologic mappers (and others) may find characterization of a feature's fractal dimension to be a useful, additional, diagnostic metric

Correspondence to:
S. J. Robbins,
stuart@boulder.swri.edu

Citation:
Robbins, S. J. (2018). The fractal nature of planetary landforms and implications to geologic mapping. *Earth and Space Science*, *5*, 211–220. https://doi.org/10.1002/2018EA000372

Received 26 JAN 2018
Accepted 2 APR 2018
Accepted article online 20 APR 2018
Published online 25 MAY 2018

The Fractal Nature of Planetary Landforms and Implications to Geologic Mapping

Stuart J. Robbins[1]

[1]Southwest Research Institute, Boulder, CO, USA

Abstract The primary product of planetary geologic and geomorphologic mapping is a group of lines and polygons that parameterize planetary surfaces and landforms. Many different research fields use those shapes to conduct their own analyses, and some of those analyses require measurement of the shape's perimeter or line length, sometimes relative to a surface area. There is a general lack of discussion in the relevant literature of the fact that perimeters of many planetary landforms are not easily parameterized by a simple aggregation of lines or even curves, but they instead display complexity across a large range of scale lengths; in fewer words, many planetary landforms are fractals. Because of their fractal nature, instead of morphometric properties converging on a single value, those properties will change based on the scale used to measure them. Therefore, derived properties can change—in some cases, by an order of magnitude or more—just when the measuring length scale is altered. This can result in significantly different interpretations of the features. Conversely, instead of a problem, analysis of the fractal properties of some landforms has led to diagnostic criteria that other remote sensing data cannot easily provide. This paper outlines the basic issue of the fractal nature of planetary landforms, gives case studies where the effects become important, and provides the recommendation that geologic mappers consider characterizing the fractal dimension of their mapped units via a relatively simple, straightforward calculation.

Plain Language Summary Planetary scientists will create geologic maps of a surface to perform different kinds of studies. Geologic maps identify features of different types and help to distill many different kinds of data into an easier to use format from which scientific investigations can be done. An analysis that is not often done, but I argue in this work should be done, is examining how mapped features vary when one uses a different measuring stick. This issue is popularized by the "infinite coastline of Britain" problem, where the coastline of Britain and, indeed, all landmasses, continuously increases the smaller one's measuring length scale gets. This concept of complexity at many different scales is the idea behind the mathematical concept of a fractal. I demonstrate in this work that fractal considerations should be factored into geologic mapping and associated analyses, for interpretations can change when phenomena like this are considered.

1. Introduction

Geologic and geomorphologic mapping (collectively "mapping" hereafter) relies on identification and tracing of the borders of different geologic and geomorphologic units (collectively "units" hereafter) and/or the tracing of linear features. From crater rims to lava flows, mountains to forests to bodies of water—while each unit and feature might be different—all rely on the identification of their boundary. From that boundary, they can be separated from adjacent units, and they can also be analyzed in and of themselves.

Often, a component of interpreting units is based on properties that are derived from perimeter traces. A straightforward measurement is area, calculated as the region enclosed by the perimeter. For some landforms, additional calculations are important, such as how far any portion of a unit extends from the center, a feature within, or a feature exterior to the unit; how large the perimeter is relative to the area; or the spatial density of the mapped features within a minimum area bounding region. As a simple, one-dimensional example, the nature of the sinuosity of rivers (actual channel length divided by the distance between the beginning and end) is closely linked to the cohesion of the material through which the water flows (e.g., Federici & Paola, 2003). In the river example, one tends to assume for simplicity that the results are scale invariant: If the length scale (in this work and common in fractal literature, length scale is "ϵ") used to measure true channel length were shortened or lengthened, the sinuosity would be the same or similar "enough" so long as a "reasonable" measuring length scale was used.

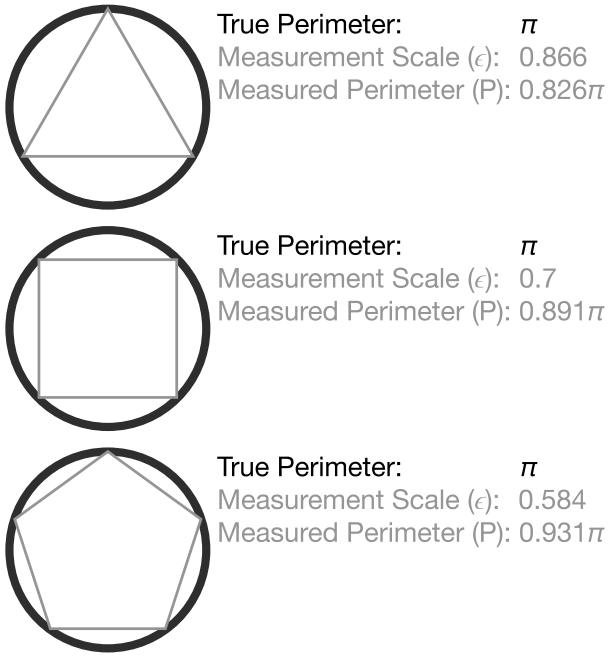

Figure 1. Simple example of how measurement length scale (ϵ) will change the perimeter (P) that is measured, though this is an instance where the perimeter could be easily parameterized by a simple curve. In this example, the shape (circle) is successively measured by different length scales that are easily circumscribed by the shape. As the length scale decreases, the measured perimeter increases, but it does not reach the true perimeter. When $\epsilon \approx 0.0628$ (100 segments), the perimeter is $\approx 0.999832\pi$.

However, this is not necessarily true, and it is a problem that was considered by L. F. Richardson over half a century ago (Richardson, 1961) and explored in significant detail by fractals pioneer Benoît B. Mandelbrot (Mandelbrot, 1967, and later works). The issue today is often colloquially known as the "coastline paradox," or more regionally, "the infinite coastline of Britain." The paradox goes as such: The measured length of the coast of a landmass will change based on how long the measuring scale is, and the shorter the scale used to measure, the longer the perimeter will be (e.g., Figure 1). Therefore, the perimeter cannot be defined as a certain length that is scale invariant. When Mandelbrot first wrote about this problem, the term "fractal" had not yet been invented (that would wait until 1975 when Mandelbrot brought together hundreds of years of work and created the term). However, the concept is now recognized as a basic fractal problem: Natural landforms are often varied such that they have complexity at every measurement scale (or at least a large range of measurement scales). Therefore, while approximations of a smooth curve or numerous straight lines might converge to a single value (or, they might not), they will never reach the "true" length because that value cannot be uniquely defined.

Returning to planetary mapping, this consideration is often ignored, and one will generally select map and measuring length scales that are reasonable given the goals of the work and/or constrained by the resolution of a base map. However, even with such a constraint, fractal considerations can—and I argue *should*—still be taken into account, for there are real applications where they can significantly affect the outcome, as this work describes in detail. Therefore, even if a mapper's specific work would not be affected, they should be cognizant of the issue and how others may use their product. The purpose of this paper is to try to resume consideration of this issue within the planetary mapping and broader planetary science communities, identify some examples of where such considerations need to be made (sections 2–3), including issues of finite resolution (section 3.5), and propose an additional measurement that might be useful in concomitant research endeavors (section 4).

2. Example: Crater Ejecta

Minimally modified impact crater ejecta across the solar system tend to display one or both of two different broad classes of morphology: On the moon and other airless bodies, ballistically emplaced ejecta transition from a thinning, continuous inner deposit to become discontinuous beyond approximately one crater radius from the crater rim and can further break into discrete rays and secondary craters. When they form, the ejecta might be the same brightness as the surrounding landscape, or they may be bright or dark. On Mars and some other bodies, the ejecta may display an abrupt terminus that is elevated from the surrounding surface, typically ≈1–1.5 crater radii from the rim, and that terminus may be in a roughly circular or flower petal-like pattern.

The extent of the ejecta deposit can be an important component of mapping—typically as a component of a generic "Cratered Unit" or "Impact Crater Unit"—but researchers who study crater ejecta typically want to characterize the ejecta further. Morphometric properties are almost exclusively derived from tracing the perimeter and deriving different metrics from that perimeter trace. These properties include perimeter, area, lobateness (perimeter divided by the circumference of a circle with the same area—analogous to channel sinuosity), the extent of the continuous ejecta from the rim (average and/or maximum), and the ratio of that extent to the crater's radius (e.g., Barlow, 1988; Mouginis-Mark, 1979; Robbins & Hynek, 2012). Except for the area, all of these metrics are affected by the fractal nature of the ejecta, sometimes significantly, as will be demonstrated in this section.

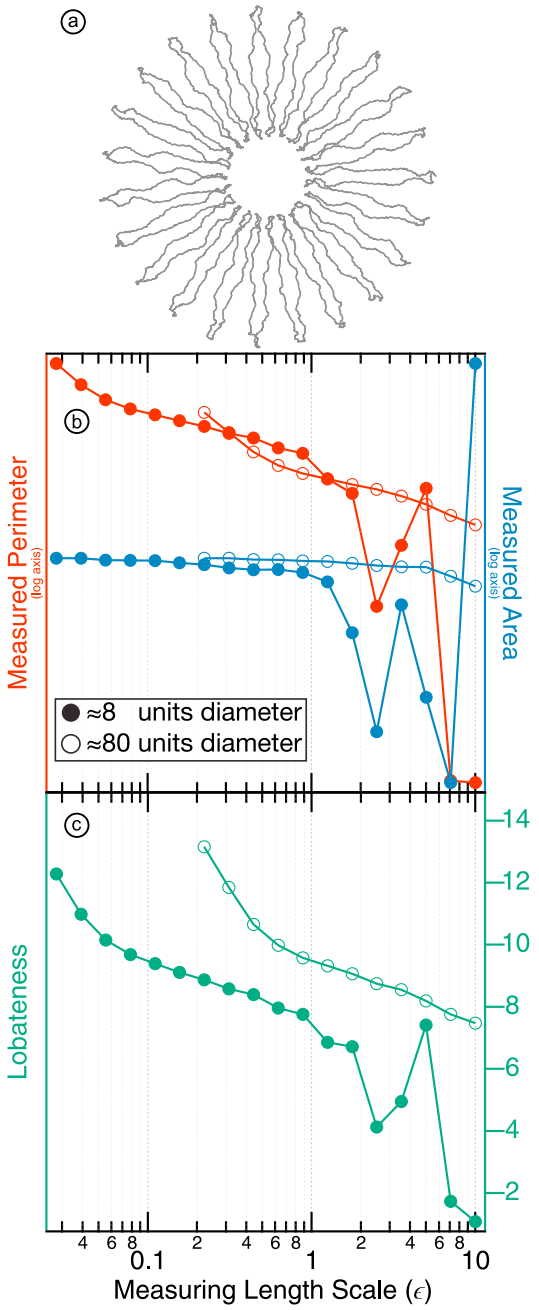

Figure 2. Simulated crater ejecta (a), the unitless measured perimeter and measured area (b), and derived lobateness (c). The modeled ejecta was created to simulate multiple scales of complexity using, as a base, the equation $r = \delta + \alpha \cdot \cos(\lambda \cdot \theta)$ where $\delta = 5$, $\alpha = 3$, and $\lambda = 23$, upon which additional, higher-frequency sine waves and Gaussian noise were added. The perimeter and area were measured using different measuring length scales where the shape was its default size (solid circles) and scaled up by 10 (open circles). Due to the computer-generated nature of the shape and Gaussian noise added to it, the scaled-up version could not be calculated to length scales as small as the default version. The perimeter and area were scaled to be the same at $\epsilon \approx 0.3$ (perimeter) and the asymptote (area). Lobateness is unitless, and so the calculated values are graphed, showing that despite the shape being the same and having the same kind of complexity, when it is larger, it will yield a larger calculated lobateness for a given ϵ due to the additionally visible complexity for a given image resolution.

However, influence of the fractal nature is rarely considered. On Mars, it was studied briefly in the published literature, with most researchers indicating Ching et al. (1993) as the first. A literature review showed only two other works on Martian impact craters that cite that study: Barlow (1994) stated that her work on Martian ejecta lobateness generally agreed with Ching et al. (1993), and Barnouin-Jha and Schultz (1998) used it to advocate that the abrupt terminus ejecta required highly nonlinear processes to form, such as turbulence in the atmosphere, because of their fractal nature. Robbins and Hynek (2012) briefly addressed the overall issue in introducing their Martian crater database, explaining that their crater lobateness data should only be compared within the database and to similarly sized craters: comparisons to other databases would be pointless due to the different measuring length scales used. On other bodies, recently, Bray et al. (2018) used fractal analysis to study lobate impact melt flows on the lunar Pierazzo crater, but this appears to be an isolated example of fractals being used in lunar crater research; the fractal analysis was focused not specifically on the crater but on crater-associated melt flows which is one of the primary applications of fractal analysis in terrestrial mapping research (see section 3). Otherwise, a literature review found that the fractal nature of crater ejecta has only otherwise been studied by a group examining ejecta on Venus (You, Kauhanen, & Raitala, 1995, 1996). It should be noted that all of these works—except Robbins and Hynek (2012) and Bray et al. (2018)—were published in the mid-1990s.

Figure 2a shows a simulated example of a complex pattern that could have properties similar to a real geologic feature. It was parameterized as a simple polar rose with numerous lobes (see figure caption), with additional high-frequency sine waves, and a small amount of Gaussian noise. Without scaling applied, the shape had a diameter of approximately 8. Figure 2b shows the measured perimeter and area of the shape (vertical axes) as different measuring length scales (ϵ) were used (horizontal axis). While area converges to a single value, there is no steady state perimeter; in fact, the perimeter increases significantly at the smallest measuring lengths due to the extra complexity at those small scales. Therefore, the calculated lobateness (Figure 2c) also changes depending on ϵ, and that change was nonlinear, not predictable, nor easily parameterized.

An additional problem of changing ϵ is that two features that are practically identical in every way except scale, such as hypothetical ejecta from a 1 km diameter crater versus 10 km diameter crater, will have different perimeter versus area properties when measured with the same length scale (e.g., $\epsilon = 10$ m). This is because the more intricate features that are resolved at 10 m for the larger crater will not resolve at 10 m for the smaller crater. Or, thought of another way, if the shape has complexity at every scale, then the larger crater will have more complexity than a smaller crater when both are measured with the same ϵ. Figure 2b illustrates this result with the example feature scaled up by a factor of 10, but keeping ϵ the same (the perimeter results are scaled to have identical values for $\epsilon \approx 0.3$, and the areas are scaled to have the same asymptotic values). The general trend is that the surface area converges more quickly, but the perimeter again has nonlinear behavior. (The nonlinear behavior occurs at different length scales, almost certainly due to the

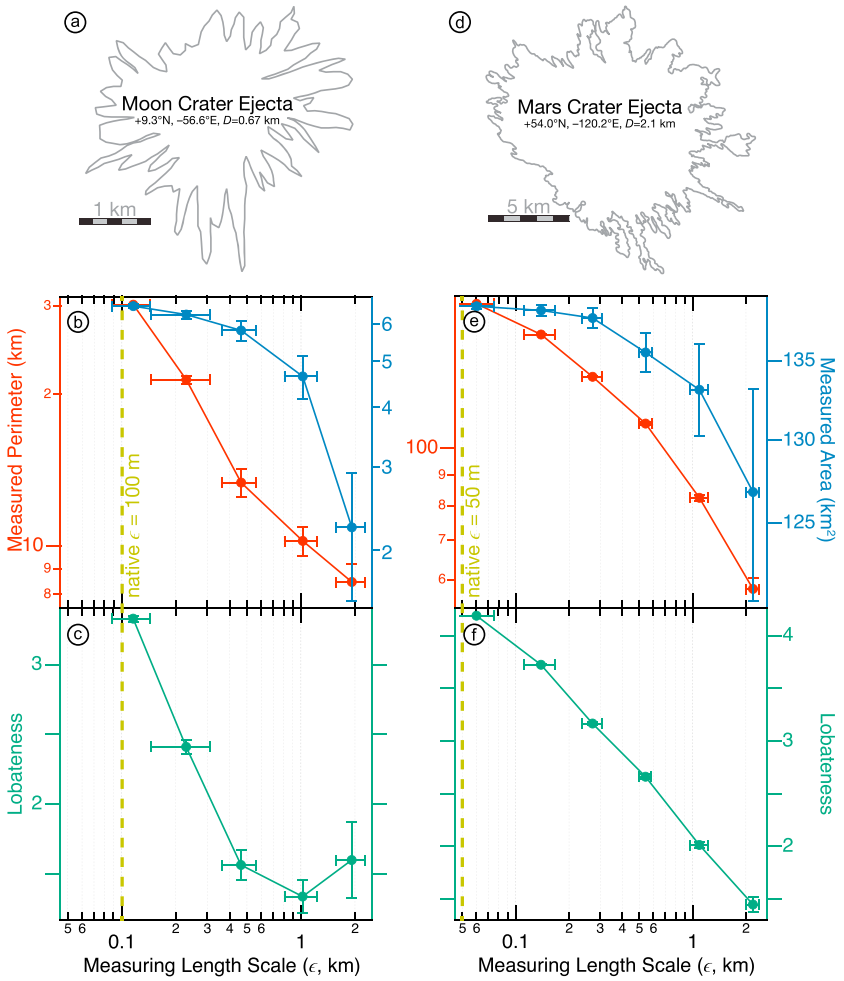

Figure 3. Same as Figure 2 but for real crater ejecta traces on the Moon (a–c) and Mars (d–f). The lunar ejecta was traced at 100 m per vertex on 30 m per pixel mosaics, and the Martian ejecta was traced at 50 m per vertex on 20 m per pixel mosaics. The lunar crater was significantly smaller than the Martian crater. Horizontal values are calculated by the average ϵ after an a priori target ϵ was set, and the horizontal error bars are the standard deviation of the resulting vertex spacing. Vertical error bars for perimeter and area are calculated from perimeter and area results when using different vertex points as the starting position from which points were removed to create different ϵ. Vertical error bars for lobateness are calculated as described in the text.

simple 10 times scaling and the shape not being a true fractal.) Therefore, the lobateness (Figure 2c) is different for a given ϵ despite the identical nature of the underlying shape; the maximum lobateness is also larger.

This is a synthetic example, and the question remains how realistic it may be. This was tested for a small bright-rayed lunar crater (D = 0.67 km) and a Martian crater (D = 2.1 km) with an abrupt ejecta terminus that displays a "splash"-like morphology, similar to bright lunar rays (Figures 3a and 3d). The bright ejecta of the lunar crater was mapped on 30 m/pixel *SELENE* Terrain Camera mosaics (Haruyama et al., 2012) with images taken near local noon, and ϵ = 100 m. The Martian crater was mapped on *Mars Reconnaissance Orbiter* Context Camera images (Malin et al., 2007) rectified and mosaicked at 20 m/pixel and traced at ϵ = 50 m, though the crater is significantly larger than the lunar example. The particular lunar crater ejecta used is relatively simple compared with many lunar bright-rayed ejecta, but this example was selected so that a reasonably accurate trace could be made without spending several hours mapping it, and it serves as a reasonable example of the phenomena discussed in this paper. Mapping was done in Environmental Systems Research Institute's geographic information system software *ArcMap*, where the measurement length scale (ϵ) is set via the "vertex spacing" parameter. At this point, I also introduce the term "native ϵ" or ϵ_{native} as the vertex spacing at which the feature was traced in software, in contrast with ϵ which may be adjusted later (e.g., horizontal axes of

Figures 2 and 3). It must also be noted that the ArcMap software that was used (version 10.3.1) had some jitter, such that ϵ_{native} = 0.103 ± 0.006 km for the lunar ejecta and ϵ_{native} = 0.056 ± 0.009 km for the Martian ejecta.

Each ejecta deposit was mapped only once, with the vertex spacing listed above. To simulate different ϵ, the ejecta trace's polygon was iteratively adjusted in software to create different and larger ϵ until a reasonably large ϵ produced an unreasonably limiting number of vertex points or unresolved feature, at which point the analysis was stopped. When the polygon was adjusted, such as when $\epsilon = 2{\cdot}\epsilon_{native}$, the process was not as simple as removing every other point. Instead, from the first point ($i = 1$), the distance ($d_{i,j}$) was calculated for each subsequent point until the distance $d_{1,N} \geq 2{\cdot}\epsilon_{native}$, and that vertex was saved and intermediate points removed. The reason for this more complicated removal is that one can envision a situation where a feature is highly complex, such that vertex $i = 2$ has a distance $d_{1,2} = \epsilon_{native}$, vertex $i = 3$ has $d_{2,3} = \epsilon_{native}$, but $d_{1,3} \neq 2{\cdot}\epsilon_{native}$ because the feature curves back on itself. Ergo, the distances must be calculated, each time, from that first point in selecting intermediate points to remove. After the second point is selected and intermediate points removed, the process was repeated. Additionally, to simulate different starting points on the ejecta (the author tends to start at the southwest point), the vertex points were shifted so that multiple starting positions for each ϵ were used. In the graphs in Figure 3, each point on the horizontal axis is the average calculated ϵ given an a priori choice for ϵ (because these are real vertex points, the final ϵ may not have exactly equaled the a priori selection), and the error bar is the standard deviation of those distances. The vertical values are based on having different starting points along the perimeter, where the displayed value is the mean and error bars are the standard deviation. For the calculated lobateness (Γ), the standard technique of adding in quadrature was used, where Δ in front of a variable indicates the measured (or calculated for Γ) uncertainty:

$$\Gamma = \frac{P}{2\pi\sqrt{A/\pi}}$$

$$\Delta\Gamma = \sqrt{\left(\frac{\delta\Gamma}{\delta P}\Delta P\right)^2 + \left(\frac{\delta\Gamma}{\delta A}\Delta A\right)^2}$$

$$\Delta\Gamma = \sqrt{\left(\frac{\delta}{\delta P}\left(\frac{P}{2\pi\sqrt{A/\pi}}\right)\Delta P\right)^2 + \left(\frac{\delta}{\delta A}\left(\frac{P}{2\pi\sqrt{A/\pi}}\right)\Delta A\right)^2}$$

$$\Delta\Gamma = \sqrt{\left(\frac{\Delta P}{2\pi\sqrt{A/\pi}}\right)^2 + \left(\frac{-P{\cdot}\Delta A}{4\pi\sqrt{A^3/\pi}}\right)^2}$$

- *Area (A)*, Figures 3b and 3e: The real examples are similar to the synthetic example in that the area tends to increase rapidly as ϵ decreases and then it reaches an asymptote. Because the few connected points for large ϵ may be very different when using different starting positions, uncertainty is relatively large.
- *Perimeter (P)*, Figures 3b and 3e: The real examples are similar to the synthetic example in that the perimeter increases as ϵ decreases. It is different in that perimeter increases consistently (though not at a constant rate) as ϵ decreases, but the synthetic example increased, flattened, and then increased again. This is likely because real ejecta are closer in nature to a real fractal—they display levels of complexity at more scales—while the synthetic example had complexity only at three scales (the primary morphology, the additional sine waves, and the Gaussian noise). Uncertainty is relatively small for each ϵ.
- *Lobateness (Γ)*, Figures 3c and 3f: Because lobateness is directly related to perimeter versus area, the lobateness is both similar and dissimilar to the synthetic example: It increases with decreasing length scale, and it increases somewhat continuously (though again, not at a constant rate).
- *Comparison between the two real ejecta*: The behavior between these two real examples is only similar in the *overall* trends: $\log(P) \propto 1/\log(\epsilon)$, $\log(\Gamma) \propto 1/\log(\epsilon)$, and $\log(A) \rightarrow$ constant as $\log(\epsilon) \rightarrow 0$. The details differ even in these two randomly chosen examples, perhaps most notably in that the lobateness of the lunar example holds nearly steady over a measuring length scale change of over half an order of magnitude, while the Martian example does not—such behavior could easily fool a researcher who did not examine the lunar ejecta's perimeter for smaller ϵ. The perimeter trend is also different between the two. For the lunar example, the perimeter increases approximately following a power law for all ϵ examined. In contrast, while the Martian ejecta's perimeter increases, that increase is at a decreasing rate on a log-log plot as ϵ

nears 0.05 km, and this could be real and not a resolution factor: While the ejecta displays fractal-like qualities at many different scales, there may be a minimum scale below-which the perimeter really is linear and the Context Camera images may resolve that at approximately few meters scale. This could be related to its formation and/or it could be due to erosion. It is also possible that it may be like the synthetic example in that it has complexity at scales $\gtrsim$few 10s m, is easily parameterized with lines near approximately tens of meter scales, and then has increasing complexity at significantly smaller (though still macroscopic) scales. Significantly more work would be necessary to determine the actual cause of this behavior and if it persists across other crater ejecta of similar morphology.

A side issue to address in this discussion of increasing perimeters versus a constant area is the phenomenon that is known in three dimensions as "Gabriel's horn" (or sometimes "Gabriel's trumpet," and less often "Torricelli's trumpet" after the seventeenth century Italian physicist and mathematician Evangelista Torricelli who studied the shape). Gabriel's horn is formed by graphing x^{-1} for $x > 0$ and rotating it about the x axis. The hyperboloid has an infinite surface area but finite volume. Reducing the dimensions by one, this is a similar issue faced with some crater ejecta where there may be some rays or ejecta components that extend very far from the crater rim, continually thinning in width and sometimes having a poorly defined maximum extent. In such a Gabriel's horn scenario, this region of the ejecta could contribute significantly to the perimeter while contributing almost nothing to the area. For example, many bright-rayed craters on the Moon and Mercury have rays that extend half-way around the body, but they are very thin in width compared to length. This is not fractal behavior because the complexity is not existent at all scales, but consideration of the phenomenon in mapping should not be overlooked.

3. Generalization to Geologic Mapping

3.1. Application to One-Dimensional Features Studied in One Dimension

The application of these issues to planetary mapping is not limited to crater ejecta. In one dimension, linear features such as tectonic faults, river valleys, and volcanic rilles need to be measured with an appropriate length scale to derive properties that are important for various studies. However, several of these kinds of features are not true fractals, for river valleys and volcanic rilles tend to have characteristic wavelengths, such that an appropriate length scale could be applied that completely parameterizes the feature.

3.2. Application to One-Dimensional Features Studied in Two Dimensions

A one-dimensional example that is analyzed in two dimensions to which fractal considerations apply is valley networks and properties associated with them, such as stream order (branching complexity, known in mathematics as the Strahler number or Horton-Strahler number), stream length, and drainage density (valleys per unit area). These three properties have important implications for the valley network and the environment in which it formed. For example, stream order is generally linked to amount of water and formation time, and drainage density can be linked to total water budgets (e.g., Hynek et al., 2010). From *Viking*-era imagery, Carr (1995) produced maps of the valley network distribution on Mars. From a new generation of spacecraft, Hynek et al. (2010) identified many more, smaller valleys that were not visible in previous imagery, resulting in 8 times more valleys, 2 times more length, 2 times higher stream order, and in some cases over 10 times higher drainage density. An implication of their work is that significantly more surface water was present on Mars when these valleys formed. In this situation, the limiting factor was primarily image resolution and quality, but the difference in the detail between the valley network maps is similar to the detail one observes when examining fractals at finer scales. For Mars, Hoke and Hynek (2009) and Hynek et al. (2010) examined limited higher-resolution images and found few additional valleys, indicating that may be the limiting scale of the fractal nature of river valleys on Mars. However, they noted that this is different from terrestrial river valleys, which continue in detail to the meter scale—hence, terrestrial river valleys can display complexity at scales spanning over five orders of magnitude. Ergo, choosing different measuring length scales will vary the end result and conclusions drawn; in some cases, this cannot be helped because appropriately high-resolution images do not yet exist (see section 3.5).

3.3. Application to Two-Dimensional Features Studied in Two Dimensions

Moving to two dimensions, crater ejecta studies are affected by the fractal nature of the ejecta. Generalizing this, ballistic and flow processes—such as lava emplacement—often display fractal-like perimeters, and

pyroclastic deposits can display the Gabriel's horn phenomenon, too. The fractal nature of lava flows were studied extensively over two decades ago primarily by Bruno et al. (1992, 1994) and Bruno and Taylor (1995), first focusing on terrestrial lavas and then applying that work to Venusian, lunar, and Martian flows. In particular, they demonstrated that plotting the measured length versus measuring scale length yielded different and potentially diagnostic power law fits (linear regressions in log space): A'ā lavas had a fractal dimension close to 1.07, and pāhoehoe 1.21 (for more on fractal dimension, see section 4). They proposed that this would apply to the extraterrestrial flows, thus giving a diagnostic tool for differentiating between lava flow types simply from analyzing the fractal nature of the mapped units—and therefore a tool for understanding the underlying material properties and geophysics. However, to date, it does not appear from a literature review as though these techniques have been applied much beyond the terrestrial volcanology community, despite much better image data sets existing now for Mars, Moon, and Mercury than were available in the 1990s; two exceptions that could be found was a conference abstract describing the work in theory (Schaefer et al., 2017) and the Bray et al. (2018) lunar study mentioned previously. Perhaps coincidentally, this initial volcanic work coincides with the bulk of the literature on fractal implications to crater ejecta.

3.4. Application to Three-Dimensional Features Studied in Three Dimensions

Expanding the application to three dimensions, the consideration moves from perimeter versus area to area versus volume. The fractal nature of landforms in three dimensions could manifest in the study of features such as mountains, and understanding the fractal nature of mountains and how they have variations at different length scales can lead to new analyses and predictions (e.g., Lehning et al., 2011). In three dimensions, continually increasing surface area versus a steady-state volume calculation can affect various analyses, such as models of radiative cooling, which are based in part on exposed surface area relative to enclosed volume. While this is a relatively minor effect compared with some other applications (some examples in this paper), it nonetheless is a real one that should be considered when not only conducting a study, but comparing that study to another that used different length scales to examine the same feature.

3.5. Issue of Data Scale and Resolution

A problem with remote sensing data is data fidelity: Whatever data are being analyzed exist at a finite resolution, and in practice, this will limit the extent of the analyzable scales. Data resolution was addressed above when describing the fractal nature of valley networks, but here it is addressed more explicitly. Fractal characterization requires analysis at a large range of scales, but that may not be possible given the data scale (physical units per pixel) or resolution (number of pixels available). There are significant practical issues here, where it is possible that one may not be able to recognize whether a feature displays fractal-like characteristics. In such cases, it is the recommendation of this paper that researchers acknowledge this potential deficit. This is also why mapping is always done as a scale-based endeavor, despite the frequent desire to analyze features below the set map scale. In the remainder of this section, three examples are discussed.

The first example is topography data. The first derivative of topography is slope, and slopes can be important in remote sensing, not the least important being characterization of landing site hazards. Slopes can also yield important information about the properties and processes of a surface, such as lava rheology or cohesion and layering of rock as it erodes, and they are often important to characterize when describing features, as in mapping. The Mars Orbiter Laser Altimeter (MOLA; Smith et al., 2001) returned 595 million altimetry points across Mars, but across-track spacing can be $>$1 km at the equator, along-track spacing is $\approx$300 m, and footprint size is 168 m. Slope maps from MOLA data show maximum slopes in Valles Marineris of ~40°; however, much higher-resolution images show overhanging cliffs (slopes $>$90°), and digital terrain models from those data will reflect this with nearly 90° slopes. In this case, the complexity and detail of the planetary landform is masked by the resolution and pixel (laser footprint) scale of the actual feature, and that detail's complexity could be of a fractal nature (complexity across a large range of scales). Given higher fidelity data, it would be wrong to claim solely from MOLA data that the maximum slopes in Valles Marineris are ~40° and draw conclusions of rock strength based on that metric. Or if that were the only dataset available, then one should provide the caveat in their analysis that slopes over smaller scales may be significantly larger.

The second example is thermal inertia data, also on Mars. Thermal inertia is effectively the resistance of a material to changes in temperature, and it has been measured with several different spacecraft, but pixel scales of various thermal inertia data are either 3 km/pixel (*Mars Global Surveyor*'s (*MGS*'s) Thermal

Emission Spectrometer (TES); Putzig et al., 2005) or at the native scale of MGS's THermal EMission Imaging Spectrometer (THEMIS; Christensen et al., 2004), roughly 100 m/pixel. While the thermal inertia maps show significant complexity, even more complexity would undoubtedly be revealed by higher-resolution data—for example, as demonstrated when comparing TES with THEMIS for the same region. For example, blocks of coherent rock have high thermal inertia, but they are more rare than well-evolved regolith and sand, which have a lower thermal inertia. Even with THEMIS, a single pixel can easily contain many scattered boulders among a field of regolith along with small patches of lower thermal inertia sand. This would all average to a single thermal inertia value, despite the large amount of complexity within the 100 × 100 pixel region. Unlike many of the other examples throughout this paper, this issue is often acknowledged in thermal inertia literature (e.g., Chojnacki et al., 2014; Edwards et al., 2009).

The final example returns to the crater ejecta studies described in section 2: If, for example, the pixels in Figure 3 were only 500 m and the practical limiting resolution for analysis were 2 pixels, then $\epsilon \geq 1$ km, and it is unlikely that one would be able to characterize the fractal nature of those two ejecta deposits. As a matter of normal scientific investigation, it is likely that a researcher would simply limit their analysis to larger craters for which the ejecta deposit—and therefore its fractal nature—could be characterized. However, there are plenty of examples in the literature of researchers pushing the resolution limits to try to extract more information.

In summary, limiting resolution effects are often—if not always—addressed in some way in planetary geologic mapping when deciding on a mapping scale and minimum feature size. However, those considerations are often not addressed during the analysis phase, after the mapping has been completed. Researchers should remember the effects of limiting resolution in the analysis stage, that there is certainly additional information hidden below the limiting pixel scale, and that information could have the potential to alter certain conclusions.

4. Discussion

The purpose of the preceding two sections is to try to reintroduce to the planetary science community, and specifically to the mapping community, the concept of fractals and related issues such as infinity (Gabriel's horn) and the interplay between data fidelity and fractal features. In section 2, a discussion of the theory, a simulated example, and two real examples of the fractal nature of ejecta deposits were examined, and section 3 described several additional examples where fractal considerations are important and how image resolution and pixel scale affect those considerations. Briefly described but not specifically discussed in those sections is the concept of a "fractal dimension," something that the community may consider to be a useful metric for characterizing mapped units. In mathematics, the fractal dimension is "dim" or simply D, but because D is often used in geologic mapping for parameters such as crater diameter, I symbolize fractal dimension as the italicized Fraktur-style D: $\mathfrak{D}$.

Fractal dimensions provide a metric to characterize the inherent complexity of a shape, and there are many methods to calculate $\mathfrak{D}$. While some methods of determining fractal dimension invoke analysis of the perimeter versus ϵ, other methods analyze the area covered by a shape versus a grid- or circle-filling approach that iteratively decreases the size of the grid. The most common of the area techniques is known as the "Minkowski-Bouligand dimension," or more commonly known simply as the descriptive "box-counting dimension." Because these are more difficult to apply and could require substantial computing power, I do not recommended them at this time.

As a simple linear example to calculate $\mathfrak{D}$, using $\epsilon = 1$, one might measure a river as having a length of $N = 3$ (length = "N" in fractal studies). If the length scale is decreased by 3 ($\epsilon = 1/3$), one would expect the same $N = 3$, but instead, it might be $N = 4$ due to the meandering nature of the river. The fractal dimension can be calculated in two ways. The first method uses only the data at that point: $\mathfrak{D} = -\log(N)/\log(\epsilon) \approx 1.262$. Alternatively, one can graph $\log(N)$ versus $\log(\epsilon)$, and the fractal dimension is 1 − slope, where "slope" is the slope of a best fit line. In this example, the plotted values would be $x = \{\log(1/3), \log(1)\} \approx \{-0.477, 0\}$ and $y = \{\log(4), \log(3)\} \approx \{0.602, 0.477\}$, such that the best fit line is $y \approx 0.477 – 0.262 \cdot x$ and the fractal dimension $\mathfrak{D} \approx 1 - (-0.262) \approx 1.262$, in agreement with the other method.

With the multiple methods to calculate the fractal dimension, it is recommended in this paper that the slope method be used; calculation at single values is prone to anomalies or outliers due to planetary landforms not

being true fractals. Using this technique, the fractal dimension of the synthetic ejecta between length scales ϵ = 0.04–0.6 is $\mathcal{D} \approx 1.11$ ($R^2 = 0.99$; this is the R^2 common to linear regressions, it is the explained variation divided by the total variation, where 0 means the fit does not explain the data and 1 means it explains all the variation; incorporation of uncertainties (from data in Figure 3 as opposed to Figure 2) can lower R^2 significantly). Over the three smallest length scales, ϵ = 0.01–0.04, the fractal dimension is $\mathcal{D} \approx 1.21$ ($R^2 = 0.98$). For the Martian ejecta, the fractal dimension for $\epsilon > 0.1$ km is $\mathcal{D} \approx 1.37$ ($R^2 = 0.58$), and for the lunar ejecta, the fractal dimension is $\mathcal{D} \approx 1.32$ ($R^2 = 0.93$). The larger fractal dimension for the Martian ejecta implies that it changes more with scale than the lunar example. In contrast, the rim of the lunar crater Copernicus was traced at ϵ_{native} = 100 m, and its fractal dimension is $\mathcal{D} \approx 1.014$ ($R^2 = 0.82$). While it is almost 1.000, it is not quite that value because it is not a perfect circle, having instead a scalloped rim. Fractal dimension is a relatively simple calculation, takes a minimum amount of computer time, can be made for any mapped unit with discrete vertex points, and could be a useful metric for researchers in the future.

A final consideration is a practical one: Despite all the examples described in this paper, the most common component of mapping in the planetary science community is the basic identification and tracing of physiographic units at a certain, singular scale, and how fractal considerations apply or could be applied is not necessarily clear. This is addressed here first in practice and then it is justified. In practice, one can use the method described in section 2 to take a unit that was mapped once and compute the fractal properties. For purpose, one might ask how could—or should—this affect perhaps the most common aspect of mapping. It is the author's opinion that the fractal nature of units will rarely affect the actual process of mapping, for most mappers are interested in the area covered by units, and areas converge quickly to a single result, such that fractal considerations would not substantively affect that result. However, mappers will often care about the perimeter of units, and in that measurement fractal considerations will come into play. Additionally, mappers usually want other researchers to use their product, and those other researchers may need to conduct analyses as discussed throughout this paper where the potential fractal nature of landforms will affect results, such as ratios of perimeter to area or feature length versus start-end distance. Additionally, as referenced with types of lava, directly characterizing the fractal nature of the perimeter can lead to important conclusions in themselves, such as helping to determine if features are similar, different, or of a certain type, which can affect the interpretation of mapped units which is usually an important component of mapping. Therefore, mappers may find it useful to consider the scales at which they map in context of complexity being present over a large variety of scales, and they may consider characterizing the fractal dimension as a component of mapping.

In summary, the community should consider revisiting the nature of fractals and their implications to planetary geologic and geomorphologic mapping and especially to studies that rely on morphometric properties of those mapped units. As illustrated in section 2, ignoring the fractal nature of features could produce erroneous results based not only on measurement length scale but also on comparing different sized features that used the same measurement scale, potentially altering the conclusions (e.g., significantly different lobateness values). Failing to consider fractal properties could also result in disagreements among researchers about measurements when, in actuality, both researchers are "correct," just at different scales. I suggest that the researchers could be "more correct" by considering a variety of measurement scales—or at least enough scales to characterize $\mathcal{D}$ of the feature(s) in question—to gain a better understanding of and appreciation for the true properties of the features and how they may or may not have multiple scales of complexity. Such scales could end up being diagnostic of the underlying physics (as in lava flows). Additionally, considering more detailed complexity that may be present at, near, or just below the resolution of planetary landforms can be an important consideration when analyzing those landforms and drawing conclusions (as in valley networks or analyzing geophysical properties where analysis is based on aggregate properties within one pixel). In conclusion, while studying the fractal nature of mapped units could in itself be an important and currently underutilized metric, a deeper understanding of and consideration for the underlying fractal nature of many landforms is an important and oft-neglected component of geologic mapping.

Acknowledgments
The author acknowledges partial support from NASA's Mars Data Analysis Program award NNX15AM48G. M. R. Kirchoff, K. Walsh, and D. Williams helped to add applications of the fractal problem (section 3), L. A. Young provided the important suggestion of starting at different locations in the polygon shape, and this paper benefited from a presubmission review by M. Chojnacki. This paper benefited from reviews by D. A. Williams and one anonymous person. All image data that was used in this work are freely available through public space agency archives: CTX data (https://pds-imaging.jpl.nasa.gov/portal/mro_mission.html) and SELENE data (https://darts.isas.jaxa.jp/planet/pdap/selene/with mosaics available at https://astrogeology.usgs.gov/maps/moon-kaguya-tc-global-mosaic).

References

Barlow, N. G. (1988). Crater size-frequency distributions and a revised Martian relative chronology. *Icarus*, *75*(2), 285–305. https://doi.org/10.1016/0019-1035(88)90006-1

Barlow, N. G. (1994). Sinuosity of Martian rampart ejecta deposits. *Journal of Geophysical Research*, *99*, 10,927–10,935. https://doi.org/10.1029/94JE00636

Barnouin-Jha, O. S., & Schultz, P. H. (1998). Lobateness of impact ejecta deposits from atmospheric interactions. *Journal of Geophysical Research*, *103*, 25,739–25,756. https://doi.org/10.1029/98JE02025

Bray, V. J., Atwood-Stone, C., Neish, C. D., Artemieva, N. A., McEwen, A. S., & McElwaine, J. N. (2018). Lobate impact melt flows within the extended ejecta blanket of Pierazzo crater. *Icarus*, *301*, 26–36. https://doi.org/10.1016/j.icarus.2017.10.002

Bruno, B. C., & Taylor, G. J. (1995). Morphologic identification of Venusian lavas. *Geophysical Research Letters*, *22*, 1897–1900. https://doi.org/10.1029/95GL01318

Bruno, B. C., Taylor, G. J., Rowland, S. K., & Baloga, S. M. (1994). Quantifying the effect of rheology on lava-flow margins using fractal geometry. *Bulletin of Volcanology*, *56*(3), 193–206. https://doi.org/10.1007/BF00279604

Bruno, B. C., Taylor, G. J., Rowland, S. K., Lucey, P. G., & Self, S. (1992). Lava flows are fractals. *Geophysical Research Letters*, *19*, 305–308. https://doi.org/10.1029/91GL03039

Carr, M. H. (1995). The Martian drainage system and the origin of valley networks and fretted channels. *Journal of Geophysical Research*, *100*, 7479–7429. https://doi.org/10.1029/95JE00260

Ching, D., Taylor, G. J., & Mouginis-Mark, P. J. (1993). Fractal dimensions of rampart impact craters on Mars (Vol. 24, pp. 283–284). Presented at the Lunar and Planetary Science Conference.

Chojnacki, M., Burr, D. M., & Moersch, J. E. (2014). Valles Marineris dune fields as compared with other Martian populations: Diversity of dune compositions, morphologies, and thermophysical properties. *Icarus*, *230*(C), 96–142. https://doi.org/10.1016/j.icarus.2013.08.018

Christensen, P. R., Jakosky, B. M., Kieffer, H. H., Malin, M. C. Jr., McSween, H. Y., Nealson, K., et al. (2004). The Thermal Emission Imaging System (THEMIS) for the Mars 2001 Odyssey Mission. In C. T. Russell (Ed.), *2001 Mars Odyssey* (pp. 85–130). Dordrecht, Netherlands: Springer. https://doi.org/10.1007/978-0-306-48600-5_3

Edwards, C. S., Bandfield, J. L., Christensen, P. R., & Fergason, R. L. (2009). Global distribution of bedrock exposures on Mars using THEMIS high-resolution thermal inertia. *Journal of Geophysical Research*, *114*, E11001. https://doi.org/10.1029/2009JE003363

Federici, B., & Paola, C. (2003). Dynamics of channel bifurcations in noncohesive sediments. *Water Resources Research*, *39*(6), 1162. https://doi.org/10.1029/2002WR001434

Haruyama, J., S. Hara, K. Hioki, A. Iwasaki, T. Morota, M. Ohtake et al. (2012). Lunar global digital terrain model dataset produced from SELENE (Kaguya) Terrain Camera stereo observations (Vol. 43, Abstract 1200). Presented at the Lunar and Planetary Science Conference.

Hoke, M. R. T., & Hynek, B. M. (2009). Roaming zones of precipitation on ancient Mars as recorded in valley networks. *Journal of Geophysical Research*, *114*, E08002. https://doi.org/10.1029/2008JE003247

Hynek, B. M., Beach, M., & Hoke, M. R. T. (2010). Updated global map of Martian valley networks and implications for climate and hydrologic processes. *Journal of Geophysical Research*, *115*, E09008. https://doi.org/10.1029/2009JE003548

Lehning, M., Grünewald, T., & Schirmer, M. (2011). Mountain snow distribution governed by an altitudinal gradient and terrain roughness. *Geophysical Research Letters*, *38*, L19504. https://doi.org/10.1029/2011GL048927

Malin, M. C., Bell, J. F. III, Cantor, B. A., Caplinger, M. A., Calvin, W. M., Clancy, R. T., et al. (2007). Context camera investigation on board the Mars Reconnaissance Orbiter. *Journal of Geophysical Research*, *112*, E05S04. https://doi.org/10.1029/2006JE002808

Mandelbrot, B. B. (1967). How long is the coast of Britain? Statistical self-similarity and fractional dimension. *Science*, *156*(3775), 636–638. https://doi.org/10.1126/science.156.3775.636

Mouginis-Mark, P. (1979). Martian fluidized crater morphology: Variations with crater size, latitude, altitude, and target material. *Journal of Geophysical Research*, *84*, 8011–8022. https://doi.org/10.1029/JB084iB14p08011

Putzig, N. E., Mellon, M. T., Kretke, K. A., & Arvidson, R. E. (2005). Global thermal inertia and surface properties of Mars from the MGS mapping mission. *Icarus*, *173*(2), 325–341. https://doi.org/10.1016/j.icarus.2004.08.017

Richardson, L. F. (1961). The problem of contiguity: An appendix to statistics of deadly quarrels. *General Systems Yearbook*, *6*, 139–187.

Robbins, S. J., & Hynek, B. M. (2012). A new global database of Mars impact craters ≥1 km: 1. Database creation, properties, and parameters. *Journal of Geophysical Research*, *117*, E05004. https://doi.org/10.1029/2011JE003966

Schaefer, E. I., Hamilton, C. W., Neish, C. D., Sori, M. M., Beard, S. P., Peters, S. I., et al. (2017). Seeing Pāhoehoe from orbit (without squinting) (Vol. 48, p. #2343). Presented at the Lunar and Planetary Science Conference.

Smith, D. E., Zuber, M. T., Frey, H. V., Garvin, J. B., Head, J. W., Muhleman, D. O., et al. (2001). Mars Orbiter Laser Altimeter: Experiment summary after the first year of global mapping of Mars. *Journal of Geophysical Research*, *106*, 23,689–23,722. https://doi.org/10.1029/2000JE001364

You, J., Kauhanen, K., & Raitala, J. (1995). Fractal properties of crater ejecta outlines on Venus. *Earth, Moon, and Planets*, *71*(1–2), 9–31. https://doi.org/10.1007/BF00612866

You, J., Kauhanen, K., & Raitala, J. (1996). Fractal properties of outflows from Venusian impact craters. *Earth, Moon, and Planets*, *73*(3), 195–214. https://doi.org/10.1007/BF00115880